On the elastic wedge problem within simplified and incomplete strain gradient elasticity theories

Yury Solyaev, Sergey Lurie, Holm Altenbach, Francesco Dell'isola

On the elastic wedge problem within simplified and incomplete strain gradient elasticity theories

Yury Solyaev [a,b,*], Sergey Lurie [a,b], Holm Altenbach [c], Francesco dell'Isola [d]

[a] Institute of Applied Mechanics of Russian Academy of Sciences, Moscow, Russia
[b] Moscow Aviation Institute, Moscow, Russia
[c] Otto-von-Guericke-Universität Magdeburg, Magdeburg, Germany
[d] Universita dell'Aquila, L'Aquila, Italy

ARTICLE INFO

Keywords:
Strain gradient elasticity
Dilatation gradient elasticity
Couple stress theory
Edge forces
Elastic wedge
Simplified gradient theories
Papkovich–Neuber solution
Singular solutions
Regularized solutions

ABSTRACT

In this paper, we investigate the behavior of the strain gradient elasticity solutions around the sharp edges of the body loaded by the concentrated loads. We consider the general Mindlin–Toupin strain gradient elasticity (SGET) and several simplified models, including the dilatation gradient elasticity theory (DGET) and the couple stress theory (CST). In the framework of a plane strain problem for an elastic wedge with prescribed tip displacement we obtain analytical assessments for the displacement field and the stress state around the wedge apex. Involving the Papkovich–Neuber solution we show that the nonsingular solutions for this problem can be obtained within the general SGET and within simplified gradient models that provide the regularization of the dilatational and the rotational parts of the displacement field both. In the incomplete theories such as DGET or CST the singularity in the displacements and stresses at the wedge apex cannot be avoided. This result is validated also based on the full-field numerical solutions for the wedge-type domains. It is shown that the stress field around the wedge apex is bounded in the complete gradient theories, while the mesh dependent solutions are realized in DGET and CST. Generally, obtained results means that the boundary value problems with the edge-type loading should be abandoned within the incomplete gradient theories like DGET and CST or it can be considered only under some additional assumptions (similarly to classical elasticity).

1. Introduction

Possibility for the explicit definition of the edge-type loading is one of the specific feature of the Mindlin–Toupin strain gradient elasticity theory (SGET) (Toupin, 1964; Mindlin, 1964), besides such famous phenomena like the description of size effects (Cordero et al., 2016; Lurie et al., 2006; Yang et al., 2020) and regularization of classical singular solutions (Gourgiotis and Georgiadis, 2009; Lazar, 2013; Sciarra and Vidoli, 2013; Lazar, 2021). However, up to date there exist not many works, in which the edge type loading is directly considered within the boundary value problems in SGET. Analysis of stress equilibrium accounting for the edge forces within SGET have been performed in application to the problems with sharp corners (Gourgiotis and Georgiadis, 2011; Gourgiotis et al., 2010) and cracks (Gourgiotis and Georgiadis, 2009; Sciarra and Vidoli, 2012). The presence of edge forces was shown to be necessary for the establishment of equilibrium in a circular sector around the tip of crack and a semi-circular sector around a concentrated force applied on a half-plane (Gourgiotis et al., 2010, 2018). Edge type boundary conditions have been investigated within the semi-inverse plane strain solutions for the rectangular domains under tension and bending (Charalambopoulos and Polyzos, 2015; Charalambopoulos et al., 2020; Placidi and El Dhaba, 2017; Solyaev and Lurie, 2021) and in three-dimensional solutions, e.g. in Giorgio et al. (2018a). Numerical simulations for the three-dimensional bodies loaded by the edge forces have been presented within SGET in Andreaus et al. (2016) and Reiher et al. (2017). Flamant and Cerutti problem for the concentrated forces acted on the half-plane have been solved within different gradient theories in Georgiadis and Anagnostou (2008), Gourgiotis et al. (2018), Anagnostou et al. (2015), Lazar and Maugin (2006) and Vasiliev et al. (2021a). Classical solutions of these problems can be found, e.g. in Lurie (2005).

In the present paper we provide an assessments for the displacement field and the stress and strain state around the sharp edge loaded by the prescribed tip displacement or concentrated force. In analytical assessments we provide an asymptotic analysis within the generalized Flamant problem, i.e. within the plain strain problem for a tip of an elastic wedge. In classical elasticity these problem for the infinite wedge

* Corresponding author at: Institute of Applied Mechanics of Russian Academy of Sciences, Moscow, Russia.
E-mail address: yos@iam.ras.ru (Y. Solyaev).

can be easily solved based on the Airy stress function approach (Barber, 2002) or by using the Mellin transform for the displacement field (Uflyand, 1965). In SGET such approaches cannot be applied since the Airy stress function is not available, while the application of the Mellin transform to SGET equilibrium equations leads to some delay differential equations, which solution is much more complicated than the initial one. Thus, in the present work we use the Papkovich–Neuber solution for the displacements, which was initially proposed in SGET by Mindlin (1964) and used, e.g. in Charalambopoulos and Polyzos (2015) and Eshel and Rosenfeld (1970). Later a simplified form of this solution was proposed and used in Lurie et al. (2011) and Solyaev et al. (2019). Based on this solution we explicitly show that the regular displacement field for the considered wedge problem can be obtained only within the general Mindlin–Toupin SGET and within simplified gradient theories that allow the regularization of the dilatation and the rotation fields both. Classical logarithmic singularity in the displacement field do not arise in such theories. Full-field solutions for the bounded wedge-type domain are also found numerically. Convergence of the mixed FEM method implemented in Comsol is shown for the considered problem within simplified SGET model with dilatation and rotation gradient effects both.

Based on the analysis of the Papkovich–Neuber solution we also show that the famous couple stress theory (CST) (Mindlin and Tiersten, 1962) and the recently proposed dilatation gradient elasticity theory (DGET) (Eremeyev et al., 2020; Lurie et al., 2021) do not allow the regular solutions around the wedge apex within the generalized Flamant problem. These theories do not provide a regular solutions for the dilatation (CST) or rotation (DGET) parts of the displacement field and corresponding classical singularities remain unavoidable in these theories. This analytical result is validated based on the numerical analysis, in which we observe the mesh dependent behavior of FE solutions obtained within CST and DGET for the bounded-domain problems. Thus, it is shown that the edge type loading cannot be prescribed explicitly within DGET and CST, since these models cannot sustain the concentrated edge forces. Corresponding discussion on the correct variational formulation of these theories can be found in Lurie et al. (2021), Madeo et al. (2016) and Park and Gao (2008).

2. Strain gradient elasticity theory

2.1. Boundary value problem

Consider an isotropic linear elastic body occupying a region Ω with a boundary $\partial\Omega$ and with edges $\partial\partial\Omega$. The strain energy density of isotropic second gradient material within Mindlin Form II is given by Mindlin (1964):

$$W(\boldsymbol{\varepsilon},\nabla\boldsymbol{\varepsilon}) = \frac{1}{2}\boldsymbol{\varepsilon} : \mathbf{C} : \boldsymbol{\varepsilon} + \frac{1}{2}\nabla\boldsymbol{\varepsilon} \vdots \mathbf{A} \vdots \nabla\boldsymbol{\varepsilon} \tag{1}$$

where $\mathbf{C}$ and $\mathbf{A}$ are the fourth- and sixth-order tensors of the elastic moduli; $\boldsymbol{\varepsilon} = \frac{1}{2}(\nabla\mathbf{u} + (\nabla\mathbf{u})^T)$ is an infinitesimal strain tensor, $\nabla\boldsymbol{\varepsilon}$ is the strain gradient tensor, $\mathbf{u}(\mathbf{x})$ is the displacements vector at a point $\mathbf{x}$; ∇ is nabla operator; and standard definitions for the scalar products $:$ and $\vdots$ are assumed accounting for the symmetries of tensors $\mathbf{C}$ and $\mathbf{A}$ (see Section 2.2).

Constitutive equations for the Cauchy stress tensor $\boldsymbol{\tau}$ and for the double stress tensor $\boldsymbol{\mu}$ (Mindlin, 1964) are given by:

$$\boldsymbol{\tau} = \frac{\partial W}{\partial \boldsymbol{\varepsilon}} = \mathbf{C} : \boldsymbol{\varepsilon}, \qquad \boldsymbol{\mu} = \frac{\partial W}{\partial \nabla\boldsymbol{\varepsilon}} = \mathbf{A} \vdots \nabla\boldsymbol{\varepsilon} \tag{2}$$

Based on the given form of the strain energy density (1) and using the variational approach the following statement of the boundary value problem of SGET can be obtained (Mindlin, 1964):

$$\begin{cases} \nabla\cdot\boldsymbol{\sigma} + \bar{\boldsymbol{b}} = 0, & \mathbf{x}\in\Omega \\ \boldsymbol{t} = \bar{\boldsymbol{t}}, \quad or \quad \mathbf{u} = \bar{\mathbf{u}}_s, & \mathbf{x}\in\partial\Omega \\ \boldsymbol{m} = \bar{\boldsymbol{m}} \quad or \quad \partial_n\mathbf{u} = \bar{\boldsymbol{g}}, & \mathbf{x}\in\partial\Omega \\ \boldsymbol{s} = \bar{\boldsymbol{s}} \quad or \quad \mathbf{u} = \bar{\mathbf{u}}_e, & \mathbf{x}\in\partial\partial\Omega \end{cases} \tag{3}$$

where $\bar{\boldsymbol{b}}$ is the volume force; $\bar{\boldsymbol{t}}$, $\bar{\boldsymbol{m}}$ are the external traction and double traction applied at the body surface $\partial\Omega$; $\bar{\boldsymbol{s}}$ is the edge traction applied at the sharp edges $\partial\partial\Omega$; $\bar{\mathbf{u}}_s$, $\bar{\mathbf{u}}_e$ define the displacements that can be prescribed at the body surface and edges, respectively; $\bar{\boldsymbol{g}}$ is the vector of normal gradients of displacements $\partial_n\mathbf{u}$ that can be prescribed on the body surface; and the definitions for the total stress tensor $\boldsymbol{\sigma}$, surface traction $\boldsymbol{t}$, surface double traction $\boldsymbol{m}$ and the edge traction $\boldsymbol{s}$ are the following:

$$\begin{aligned} &\boldsymbol{\sigma} = \boldsymbol{\tau} - \nabla\cdot\boldsymbol{\mu}, \\ &\boldsymbol{t} = \mathbf{n}\cdot\boldsymbol{\sigma} - \nabla_S\cdot(\mathbf{n}\cdot\boldsymbol{\mu}) - H\,\mathbf{nn} : \boldsymbol{\mu}, \\ &\boldsymbol{m} = \mathbf{nn} : \boldsymbol{\mu}, \\ &\boldsymbol{s} = \left[\mathbf{n}\boldsymbol{\nu} : \boldsymbol{\mu}\right] \end{aligned} \tag{4}$$

where $\nabla_S = \nabla - \mathbf{n}\partial_n$ is the surface gradient operator; $H = -\nabla_S\cdot\mathbf{n}$ is twice the mean curvature of $\partial\Omega$; $\mathbf{n}$ is the unit outward normal vector on the boundary $\partial\Omega$; $\boldsymbol{\nu} = \mathbf{n}\times\mathbf{v}$ is the co-normal vector, which is tangent to the surface $\partial\Omega$ and normal to the edge $\partial\partial\Omega$; $\mathbf{v}$ is the tangent vector to edge $\partial\partial\Omega$; and square brackets [...] denote the difference between enclosed values evaluated from the both sides of given edge.

Conditions for the edge tractions and displacements that explicitly persist in the SGET boundary value problem is the subject of the present research. In general formulation of SGET these conditions follow from the variational approach (dell'Isola et al., 2017).

2.2. Constitutive equations

Components of the constitutive tensors $\mathbf{C}$ and $\mathbf{A}$ within Mindlin Form II can be defined as follows (dell'Isola et al., 2009; Lazar et al., 2021):

$$C_{ijkl} = C_{jikl} = C_{ijlk} = C_{klij} = \lambda\delta_{ij}\delta_{kl} + \mu(\delta_{ik}\delta_{jl} + \delta_{il}\delta_{jk}) \tag{5}$$

$$\begin{aligned} A_{ijklmn} &= A_{jiklmn} = A_{ijkmln} = A_{lmnijk} \\ &= a_1(\delta_{ij}\delta_{kl}\delta_{mn} + \delta_{in}\delta_{jk}\delta_{lm} + \delta_{ij}\delta_{km}\delta_{ln} + \delta_{ik}\delta_{jn}\delta_{lm}) \\ &+ a_2\,\delta_{ij}\delta_{kn}\delta_{lm} \\ &+ a_3(\delta_{ik}\delta_{jl}\delta_{mn} + \delta_{im}\delta_{jk}\delta_{ln} + \delta_{ik}\delta_{jm}\delta_{ln} + \delta_{il}\delta_{jk}\delta_{mn}) \\ &+ a_4(\delta_{il}\delta_{jm}\delta_{kn} + \delta_{im}\delta_{jl}\delta_{kn}) \\ &+ a_5(\delta_{il}\delta_{jn}\delta_{km} + \delta_{im}\delta_{jn}\delta_{kl} + \delta_{in}\delta_{jl}\delta_{km} + \delta_{in}\delta_{jm}\delta_{kl}) \end{aligned} \tag{6}$$

where λ, μ are the classical Lame constants and a_i (i=1...5) are the additional material constants of gradient theory, that can be found, e.g. based on the interatomic potentials or via ab initio calculations (Lazar et al., 2021); δ_{ij} is the Kronecker delta.

Components of the Cauchy stresses $\boldsymbol{\sigma}$ and the double stresses $\boldsymbol{\mu}$ (2) become:

$$\tau_{ij} = \tau_{ji} = \lambda\delta_{ij}\varepsilon_{ll} + 2\mu\varepsilon_{ij} \tag{7}$$

$$\begin{aligned} \mu_{ijk} = \mu_{jik} &= a_1(2\delta_{ij}\varepsilon_{kl,l} + \delta_{ik}\varepsilon_{ll,j} + \delta_{jk}\varepsilon_{ll,i}) + a_2\delta_{ij}\varepsilon_{ll,k} \\ &+ 2a_3(\delta_{jk}\varepsilon_{il,l} + \delta_{ik}\varepsilon_{jl,l}) + 2a_4\varepsilon_{ij,k} + 2a_5(\varepsilon_{jk,i} + \varepsilon_{ik,j}), \end{aligned} \tag{8}$$

where $\varepsilon_{ij} = \varepsilon_{ji}$ are the components of infinitesimal strain tensor, $\varepsilon_{ij,k}$ are the components of the strain gradient tensor; and repeated indexes imply summation.

2.3. Solution for equilibrium equations

Substituting constitutive Eqs. (7), (8) into $(3)_1$ one can obtain the form of the equilibrium equations in terms of displacements. In absence of body forces (that is of interest for the following analysis) we obtain (Mindlin (1964)):

$$(\lambda+2\mu)(1-l_1^2\nabla^2)\nabla\nabla\cdot\mathbf{u} - \mu(1-l_2^2\nabla^2)\nabla\times\nabla\times\mathbf{u} = 0 \tag{9}$$

where

$$l_1^2 = \frac{4a_1 + a_2 + 4a_3 + 2a_4 + 4a_5}{\lambda+2\mu}, \qquad l_2^2 = \frac{a_3 + a_4 + a_5}{\mu}$$

are the length scale parameters of isotropic elastic material, which arise in the equilibrium equations of Mindlin–Toupin strain gradient elasticity.

Papkovich–Neuber solution for the equilibrium Eqs. (9) can be presented in the following form (Lurie et al., 2011; Solyaev et al., 2019):

$$\begin{aligned}&\mathbf{u} = \mathbf{u}^{(c)} + \mathbf{u}^{(g)},\\ &\mathbf{u}^{(c)} = \boldsymbol{\Phi} - \kappa\nabla(\mathbf{x}\cdot\boldsymbol{\Phi}),\\ &\mathbf{u}^{(g)} = l_1^2\nabla\psi + \boldsymbol{\Psi} - l_2^2\nabla\nabla\cdot\boldsymbol{\Psi}\end{aligned} \tag{10}$$

where $\mathbf{u}^{(c)}$ is the classical part of the solution, which is defined through the classical Papkovich–Neuber harmonic vector potential $\boldsymbol{\Phi}$ and classical parameter $\kappa = \frac{\lambda+\mu}{2(\lambda+2\mu)}$; classical scalar potential is omitted here assuming that the material Poisson's ratio does not equal to 0.25 (Lurie, 2005); $\mathbf{u}^{(g)}$ is the gradient part of the solution that is defined through the scalar potential ψ and vector potential $\boldsymbol{\Psi}$.

Classical vector potential should satisfy the Laplace equation (like in classical elasticity (Lurie, 2005)):

$$\nabla^2\boldsymbol{\Phi} = 0 \tag{11}$$

while the gradient potentials should obey the Helmholtz equations of the following form:

$$\boldsymbol{\Psi} - l_2^2\nabla^2\boldsymbol{\Psi} = 0, \qquad \psi - l_1^2\nabla^2\psi = 0 \tag{12}$$

Validity of the presented form of general solution (10)–(12) can be checked by its direct substitution into governing Eqs. (9). This form of general solution can be also obtained from those one developed by Mindlin (1964). Note, that in the Mindlin's solution he used the vector and the scalar potentials that satisfies the fourth-order equations with differential operator $(1 - l_i^2\nabla^2)\nabla^2$. Taking into account that the general solution for such equations can be presented as the sum of general solutions for the equation with the Laplace operator ∇^2 and for the equation with the Helmholtz operator $(1 - l_i^2\nabla^2)$ one will come to the form of the solution given by (10)–(12). For example, the vector potential $\boldsymbol{\Psi}$ used in the present formulation will coincides with the Mindlin's auxiliary vector potential $\boldsymbol{B}''$.

Solution form (10)–(12) was proposed in Lurie et al. (2011) and used, e.g. in the micromechanics problems in Solyaev et al. (2019). Based on this representation, the numerical Trefftz method for SGET problems was developed in Lurie et al. (2006) and Solyaev and Lurie (2021).

As it is seen from (10)–(12), the gradient potentials ψ and $\boldsymbol{\Psi}$ define the irrotational (longitudinal) and the rotational (transverse) parts of gradient displacements $\mathbf{u}^{(g)}$, respectively. Indeed, evaluating the divergence and the curl of $\mathbf{u}^{(g)}$ we find

$$\begin{aligned}&\nabla\cdot\mathbf{u}^{(g)} = l_1^2\nabla^2\psi,\\ &\nabla\times\mathbf{u}^{(g)} = \nabla\times\boldsymbol{\Psi}\end{aligned} \tag{13}$$

Therefore, the gradient part of dilatation $\Theta_g = \nabla\cdot\mathbf{u}^{(g)}$ and the gradient part of rotation $\boldsymbol{w}_g = \frac{1}{2}\nabla\times\mathbf{u}^{(g)}$ are given by:

$$\begin{aligned}&\Theta_g = \psi,\\ &\boldsymbol{w}_g = \frac{1}{2}\nabla\times\boldsymbol{\Psi},\end{aligned} \tag{14}$$

where we take into account that the scalar potential ψ obeys the Helmholtz equation.

From this result it follows at first, that the scalar potential ψ has an explicit physical meaning because it defines the gradient part of the material dilatation Θ_g, while $\boldsymbol{\Psi}$ is the vector potential for the rotational part of gradient displacements $\boldsymbol{w}_g$ (moreover, it can be shown that $\boldsymbol{\Psi} = -2l_2^2\nabla\times\boldsymbol{w}_g$).

Secondly, from (14) it follows that we can use the divergence-free vector potential $\boldsymbol{\Psi}$ to define the general solution for gradient displacements $\mathbf{u}^{(g)}$. This proposition can be additionally justified by the following reasoning. It is known that the general solution for the vector Helmholtz equation can be decomposed into the sum of the longitudinal (potential) part $\boldsymbol{\Psi}_L$ and the transverse (solenoidal) part $\boldsymbol{\Psi}_T$ as follows (Morse and Feshbach, 1953)

$$\begin{aligned}&\boldsymbol{\Psi} = \boldsymbol{\Psi}_L + \boldsymbol{\Psi}_T\\ &\boldsymbol{\Psi}_L = \nabla f, \quad f - l_2^2\nabla^2 f = 0, \quad \nabla\cdot\boldsymbol{\Psi}_T = 0\end{aligned} \tag{15}$$

where f is some scalar function that obeys the scalar Helmholtz equation and the structure of transverse part $\boldsymbol{\Psi}_T$ will be discussed below for the particular case of polar cylindrical coordinates.

Substituting (15) into the third equation in (10) we can check that gradient displacements do not depend on the longitudinal part $\boldsymbol{\Psi}_L$ and that the term $\nabla\nabla\cdot\boldsymbol{\Psi}$ can be also neglected in this case:

$$\begin{aligned}\mathbf{u}^{(g)} &= l_1^2\nabla\psi + \boldsymbol{\Psi}_T - l_2^2\nabla\nabla\cdot\boldsymbol{\Psi}_T + \boldsymbol{\Psi}_L - l_2^2\nabla\nabla\cdot\boldsymbol{\Psi}_L\\ &= l_1^2\nabla\psi + \boldsymbol{\Psi}_T - l_2^2\cancel{\nabla\nabla\cdot\boldsymbol{\Psi}_T} + \cancel{\nabla(f - l_2^2\nabla^2 f)}\end{aligned} \tag{16}$$

Thus, for the Papkovich–Neuber solution in SGET we can use the divergence-free vector potential $\boldsymbol{\Psi} \equiv \boldsymbol{\Psi}_T$ and the representation of $\mathbf{u}^{(g)}$ will be reduced to the standard Helmholtz decomposition. This will significantly simplify the form of the solution because we can use the limited number of terms in representations of $\boldsymbol{\Psi}$.

Also let as additionally clarify the meaning of the gradient part of dilatation Θ_g and the rotation $\boldsymbol{w}_g$ and representations (14). Taking the divergence and the curl of equilibrium Eqs. (9) we found that the total dilatation $\Theta = \nabla\cdot\mathbf{u}$ and rotation $\boldsymbol{w} = \frac{1}{2}\nabla\times\mathbf{u}$ should obey the following fourth order equations:

$$(1 - l_1^2\nabla^2)\nabla^2\Theta = 0 \tag{17}$$

$$(1 - l_2^2\nabla^2)\nabla^2\boldsymbol{w} = 0 \tag{18}$$

Solution of these equations can be decomposed into the sum of the solutions for the Laplace and Helmholtz equations as follows:

$$\Theta = \Theta_g + \Theta_c, \qquad \boldsymbol{w} = \boldsymbol{w}_g + \boldsymbol{w}_c \tag{19}$$

$$\nabla^2\Theta_c = 0, \qquad \nabla^2\boldsymbol{w}_c = 0 \tag{20}$$

$$(1 - l_1^2\nabla^2)\Theta_g = 0, \qquad (1 - l_2^2\nabla^2)\boldsymbol{w}_g = 0 \tag{21}$$

where gradient fields Θ_g and $\boldsymbol{w}_g$ are introduced in (14), while $\Theta_c = \nabla\cdot\mathbf{u}^{(c)}$ and $\boldsymbol{w}_c = \frac{1}{2}\nabla\times\mathbf{u}^{(c)}$ are the classical parts of dilatation and rotation; and it can be easily checked that relations (20), (21) can be satisfied identically taking into account (10)–(12), (14).

2.4. Papkovich-Neuber solution in polar cylindrical coordinates

In the following we will consider the plain strain problems in polar cylindrical coordinates, for which we will use the notations $r \in [0,\infty]$, $\theta \in [0, 2\pi]$, and the out-of-plane axis is $z \in [-\infty,\infty]$. Formulation of SGET equations for the orthogonal curvilinear coordinates in terms of covariant derivatives can be found, e.g. in Zhao and Pedroso (2008). For the plain strain formulation we assume that the third component of the displacement vector equals to zero $u_z \equiv 0$ and that all field variables do not depend on the coordinate z. In this case, the formulation of the model is the same as presented, while only two of three equilibrium equations are non-trivial, surface boundary conditions will reduce to lines, and edge boundary conditions will reduce to the corner points of the body projection on the $r\theta$-plane.

Components of the displacement field according to the Papkovich–Neuber representation (10) in polar coordinates have the following form (all relations in this paper will be given in terms of physical components of vectors and tensors):

$$\begin{aligned}&u_r^{(c)} = (1-\kappa)\Phi_r - r\kappa\frac{\partial\Phi_r}{\partial r}\\ &u_\theta^{(c)} = \Phi_\theta - \kappa\frac{\partial\Phi_r}{\partial\theta}\\ &u_r^{(g)} = \Psi_r + l_1^2\frac{\partial\psi}{\partial r}\\ &u_\theta^{(g)} = \Psi_\theta + \frac{l_1^2}{r}\frac{\partial\psi}{\partial\theta}\end{aligned} \tag{22}$$

where we assume that the vector field $\boldsymbol{\Psi} = \{\Psi_r, \Psi_\theta, 0\}$ is solenoidal as discussed above.

Classical potential $\boldsymbol{\Phi} = \{\Phi_r, \Phi_\theta, 0\}$ should obey the vector Laplace equation, which solution in polar coordinates can be presented in the following series form (see, e.g. Quartapelle (2013)):

$$\begin{aligned}
\Phi_r =& c_{10}\ln r\sin\theta + c_{30}\sin\theta + c_{50}\ln r\cos\theta + c_{70}\cos\theta \\
&+ \sin\theta\left(\sum_{n=1}^{\infty} r^{-n}(c_{1n}\cos n\theta + c_{2n}\sin n\theta) + r^{n}(c_{3n}\cos n\theta + c_{4n}\sin n\theta)\right) \\
&+ \cos\theta\left(\sum_{n=1}^{\infty} r^{-n}(c_{5n}\cos n\theta + c_{6n}\sin n\theta) + r^{n}(c_{7n}\cos n\theta + c_{8n}\sin n\theta)\right) \\
\Phi_\theta =& c_{10}\ln r\cos\theta + c_{30}\cos\theta - c_{50}\ln r\sin\theta - c_{70}\sin\theta \\
&+ \cos\theta\left(\sum_{n=1}^{\infty} r^{-n}(c_{1n}\cos n\theta + c_{2n}\sin n\theta) + r^{n}(c_{3n}\cos n\theta + c_{4n}\sin n\theta)\right) \\
&- \sin\theta\left(\sum_{n=1}^{\infty} r^{-n}(c_{5n}\cos n\theta + c_{6n}\sin n\theta) + r^{n}(c_{7n}\cos n\theta + c_{8n}\sin n\theta)\right)
\end{aligned} \tag{23}$$

where c_{mn} ($m = 1..8$, $n = 0...\infty$) are the unknown constants to be determined from the boundary conditions of the problem.

Divergence-free solution for the vector Helmholtz equation in polar coordinates can be defined as follows (Morse and Feshbach, 1953):

$$\boldsymbol{\Psi} \equiv \boldsymbol{\Psi}_T = l_2^2\nabla\times\nabla\times(\mathbf{r}\chi), \quad i.e. \quad \Psi_r = \frac{l_2^2}{r}\frac{\partial^2\chi}{\partial\theta^2}, \quad \Psi_\theta = -l_2^2\frac{\partial^2\chi}{\partial r\partial\theta} \tag{24}$$

where we neglect the part of the solution that defines the out-of-plain displacements (this part has the form $\nabla\times(\mathbf{r}\chi)$); $\mathbf{r}$ is the position vector and χ is some scalar function that satisfies the Helmholtz equation:

$$\chi - l_2^2\nabla^2\chi = 0 \tag{25}$$

Solutions for the scalar Helmholtz equations is needed then to define function ψ that is introduced in the initial form of the Papkovich–Neuber solution (10) and function χ that is used in (24), (25). These solutions can be presented as follows:

$$\begin{aligned}
\psi &= \sum_{n=0}^{\infty}\left(K_n\left(\frac{r}{l_1}\right)(b_{1n}\cos n\theta + b_{2n}\sin n\theta) + I_n\left(\frac{r}{l_1}\right)(b_{3n}\cos n\theta + b_{4n}\sin n\theta)\right) \\
\chi &= \sum_{n=0}^{\infty}\left(K_n\left(\frac{r}{l_2}\right)(d_{1n}\cos n\theta + d_{2n}\sin n\theta) + I_n\left(\frac{r}{l_2}\right)(d_{3n}\cos n\theta + d_{4n}\sin n\theta)\right)
\end{aligned} \tag{26}$$

where b_{mn}, d_{mn} are the unknown constants; and K_n and I_n are the modified Bessel functions.

Thus, we represent the classical part of general solution $\mathbf{u}^{(c)}$ via two components of the harmonic vector potential Φ_r, Φ_θ (23). The gradient part of the solution $\mathbf{u}^{(g)}$ is defined through the two scalar functions χ and ψ (26).

The completeness of the presented form of the solution can be claimed based on the following reasoning (though the rigorous mathematical proof we remain for the future work):

(1) The validity of additive decomposition of the displacement solution into the classical part $\mathbf{u}^{(c)}$ and gradient part $\mathbf{u}^{(g)}$ in (10) follows, e.g. from the known form of the Green's functions developed within three-dimensional and plane problems of SGET (Gourgiotis et al., 2018; Ma et al., 2018).

(2) Classical part of the solution $\mathbf{u}^{(c)}$ satisfies the classical equilibrium equations. For this part of the solution we use the standard Papkovitch–Neuber representation in (10), which completeness in the static case have been shown in classical elasticity (see Mindlin (1936), Gurtin (1962) and Lurie (2005)).

(3) As it is shown in (15), (16), representation for the gradient part of solution $\mathbf{u}^{(g)}$ in (10) is equivalent to the standard Helmholtz decomposition of the vector field. Restrictions of the Helmholtz decomposition are that the vector field should be sufficiently smooth and that in the unbounded domains it should decay faster then r^{-1} (Sprössig, 2010). In SGET, gradient part of solution $\mathbf{u}^{(g)}$ defines the boundary layers effect that undergoes exponential decay (Gourgiotis et al., 2018; Solyaev et al., 2019; Ma et al., 2018). Moreover, in the further analysis we will not consider the unbounded domains. We will restrict our analysis only for the area around the wedge apex.

(4) Scalar potentials in (22), (24), (25) obey the Laplace and Helmholtz equations. Completeness of series representation for these potentials (23), (26) was proven in the context of Trefftz method (see Zieliński (1995) and references therein). These series representations can be used for the domains without re-entrant corners. For angle singularities one should include additionally the so-called special purpose functions (like terms with radial functions $r^{-n+\xi}$, $K_{n+\xi}(r)$, where ξ is some real number) (Zieliński, 1995; Kołodziej and Zielinski, 2009). Thus, in the following analysis we will consider only the domains with external edges and we will use series (23) and (26). Re-entrant corners will be out of consideration. Such problems within gradient theories were considered in Gourgiotis and Georgiadis (2011) and Gourgiotis et al. (2010) for the remotely applied loading.

In the next subsections we will consider three simplified gradient theories and discuss the form of the general solutions for the governing equations of these theories. The difference between these theories lies in the assumptions about the structure of the gradient elastic moduli tensor (6) and the double stress tensor (8). Representations of the Cauchy stress tensor (7) are all the same in these theories.

2.5. Simplified strain gradient elasticity theory

Simplified strain gradient elasticity theory (SSGET) contains single additional length scale parameter. This theory have been widely investigated in last decades (Askes and Aifantis, 2011; Eremeyev et al., 2019). Constitutive assumptions in SSGET are the following (Altan and Aifantis, 1997; Lazar and Maugin, 2005):

$$a_1 = a_3 = a_5 = 0, \qquad a_2 = \lambda l^2, \qquad a_4 = \mu l^2, \qquad l_1 = l_2 = l \tag{27}$$

Using this assumption in (8) one can obtain the following definition for the double stress tensor:

$$\mu_{ijk} = \mu_{jik} = l^2\tau_{ij,k} = \lambda l^2\delta_{ij}\varepsilon_{ll,k} + 2\mu l^2\varepsilon_{ij,k} \tag{28}$$

and the simplified form of the governing equations:

$$(1 - l^2\nabla^2)\big((\lambda + 2\mu)\nabla\nabla\cdot\mathbf{u} - \mu\nabla\times\nabla\times\mathbf{u}\big) = 0 \tag{29}$$

General solution of SGET can be represented as it was done above for the general theory (10)–(12) in 3D case or by using (22)–(26) for 2D problems in polar cylindrical coordinates. The form of this solution will be the same as for the general Mindlin–Toupin theory, however one should use the single length scale parameter $l = l_1 = l_2$.

One should also note, that in the present study we used SSGET with rigorous formulation of boundary conditions that follows from the variational principle according to the initial Mindlin's and Toupin's works (Toupin, 1964; Mindlin, 1964). Some erroneous simplifications of the boundary conditions within SSGET have been introduced previously (Askes and Aifantis, 2011) that may leads to the non-correct solutions (see, e.g. Lazar and Polyzos (2015)).

2.6. Dilatation gradient elasticity theory

Constitutive relations of DGET include the single non-zero gradient modulus as follows (Lurie et al., 2021):

$$a_1 = a_3 = a_4 = a_5 = 0, \qquad a_2 = (\lambda + 2\mu)l^2 \tag{30}$$

Substituting (30) into (8), we obtain the double stress tensor:

$$\mu_{ijk} = \mu_{jik} = (\lambda + 2\mu)l^2\delta_{ij}\varepsilon_{ll,k} \tag{31}$$

and governing Eqs. (9) in DGET become to:

$$(\lambda+2\mu)(1-l^2\nabla^2)\nabla\nabla\cdot\mathbf{u}-\mu\nabla\times\nabla\times\mathbf{u}=0 \tag{32}$$

In DGET, the gradient part of the displacement solution $\mathbf{u}^{(g)}$ is irrotational. Namely, it can be seen that the solenoidal vector $\boldsymbol{\Psi}$ in the Papkovich–Neuber solution of the general theory (10) does not satisfy the governing equations of DGET (32). Thus, the general solution of DGET can be represented using purely potential field of gradient displacements as follows:

$$\begin{aligned}&\mathbf{u}=\mathbf{u}^{(c)}+\mathbf{u}^{(g)},\\&\mathbf{u}^{(c)}=\boldsymbol{\Phi}-\kappa\nabla(\mathbf{x}\cdot\boldsymbol{\Phi}),\qquad \mathbf{u}^{(g)}=l^2\nabla\psi,\\&\nabla^2\boldsymbol{\Phi}=0\qquad \psi-l^2\nabla^2\psi=0\end{aligned} \tag{33}$$

Peculiarity of this representation (33) is that the scalar potential ψ that defines the gradient part of the displacement function at the same time defines the gradient part of the material dilatation $\Theta_g=\nabla\cdot\mathbf{u}_g=\psi$ (see (14)). Rotation vector in DGET does not contain the gradient part, i.e. $\boldsymbol{w}^{(g)}\equiv 0$, $\boldsymbol{w}=\boldsymbol{w}^{(c)}$. General solution for the scalar potential ψ is given by series representation in Eqs. (26). Components of classical vector potential $\boldsymbol{\Phi}$ are given by Eqs. (23).

2.7. Couple stress theory

Formulation of the couple stress theory (CST) can be obtained from the Mindlin Form II if one assumes (dell'Isola et al., 2009):

$$\begin{aligned}&a_1=2l^2\eta\mu,\quad a_2=-4l^2\eta\mu,\quad a_3=-l^2\eta\mu,\\&a_4=2l^2(\eta+1)\mu,\quad a_5=-l^2(\eta+1)\mu,\quad l_1=0,\quad l_2=l\end{aligned} \tag{34}$$

where $-1<\eta<1$. Substituting (34) into (8), the double stress tensor in CST takes the form:

$$\mu_{ijk}=\mu_{jik}=2\mu l^2\Big(2\eta(2\delta_{ij}\omega_{kp,p}-\delta_{ik}\omega_{jp,p}-\delta_{jk}\omega_{ip,p})+(1+\eta)(\omega_{ik,j}+\omega_{jk,i})\Big), \tag{35}$$

where $\omega_{ij}=(u_{i,j}-u_{j,i})/2$ is the infinitesimal rotation tensor.

The governing Eqs. (9) in CST become to

$$(\lambda+2\mu)\nabla\nabla\cdot\mathbf{u}-\mu(1-l^2\nabla^2)\nabla\times\nabla\times\mathbf{u}=0 \tag{36}$$

As it is easy to see, the potential part of the general Papkovtich–Neuber solution $\nabla\psi$ will not satisfy the governing equations of CST (36). Thus, in opposite to DGET, gradient part of the displacement field in CST does not contain the potential part and consist only of the transverse part. In other words, the dilatation remains classical in the CST and $\Theta_g\equiv 0$, $\Theta=\Theta_c$. Papkovtich–Neuber solution of CST can be represented as the particular case of general relations (10), (24), (25) and in polar coordinates it has the following form:

$$\begin{aligned}&\mathbf{u}=\mathbf{u}^{(c)}+\mathbf{u}^{(g)},\\&\mathbf{u}^{(c)}=\boldsymbol{\Phi}-\kappa\nabla(\mathbf{x}\cdot\boldsymbol{\Phi}),\qquad \mathbf{u}^{(g)}=\boldsymbol{\Psi}\\&\nabla^2\boldsymbol{\Phi}=0,\quad \boldsymbol{\Psi}=l^2\nabla\times\nabla\times(\mathbf{r}\chi),\quad \chi-l^2\nabla^2\chi=0\end{aligned} \tag{37}$$

More complex form of the general solution within CST have been developed by Mindlin in Mindlin and Tiersten (1962) and used in Gourgiotis and Georgiadis (2011). However, following the same procedure as was described in Section 2.3 of this paper and assuming the absence of the external forces it can be easily shown, that the Mindlin's solution for CST equilibrium equations for the plain strain problems in cylindrical polar coordinates can be reduced to the presented one (37).

Thus, we consider three simplified variants of gradient elasticity theories and we will use them in the next section within the elastic wedge problem. In DGET we have purely potential field of gradient displacements (33). In CST this field is purely solenoidal (37). In SSGET the gradient part of displacements have the potential and the rotational parts both similarly to the general Mindlin–Toupin strain gradient elasticity (10). These properties of the displacement fields are the consequence of the constitutive assumptions (27), (30), (34) and corresponding form of equilibrium equations of these models.

Note, that the constitutive assumptions of DGET and CST lay on the border of the permissible assumptions that provides the positive definiteness of the stored elastic energy within SGET (see dell'Isola et al. (2009) and Lurie et al. (2021)). Therefore, these theories (DGET and CST) are the semi-positive definite particular cases of SGET. That's why we call these theories as "incomplete".

3. Elastic wedge loaded by tip displacement

Let us consider an elastic wedge bounded by two edges $\theta=\pm\alpha$ ($\alpha\le\pi/2$) and loaded at the apex by the tip displacement $\bar{u}_1$ prescribed in the horizontal direction ($\theta=\pi$). The illustration is given in Fig. 1. Polar coordinates are defined with the origin at the wedge apex. Angle coordinate is evaluated from the reference direction that divides the wedge into two symmetrical parts.

Classical elasticity solution for the similar problem with prescribed concentrated force (generalized Flamant problem) can be developed based on the Airy stress function approach (Barber, 2002). In this solution for the symmetric type of the loading the stresses are given by:

$$\tau_{rr}^{clas}=\frac{2F}{2\alpha+\sin 2\alpha}\frac{\cos\theta}{r},\quad \tau_{r\theta}^{clas}=\tau_{\theta\theta}^{clas}=0 \tag{38}$$

where F is the prescribed force at the wedge apex.

Classical displacement solution for the symmetric loading have the following form:

$$\begin{aligned}u_r^{clas}&=C_1\theta\sin\theta-C_2\cos\theta+C_3\ln r\cos\theta\\u_\theta^{clas}&=C_1\theta\cos\theta-C_2\sin\theta-C_3\ln r\sin\theta\end{aligned} \tag{39}$$

where $C_1=\frac{C}{2(\lambda+\mu)}$, $C_2=\frac{C}{4\mu}$, $C_3=\frac{C}{4\kappa\mu}$, $C=\frac{F}{2\alpha+\sin 2\alpha}$.

Note, that these solution (39) in classical elasticity can be also derived by using the Papkovich–Neuber potentials. To do it one should remain only two non-zero coefficients c_{50} and c_{70} in series representation for the classical vector potential $\boldsymbol{\Phi}$ in (23). Also to this potential one should add the term of the form

$$\begin{aligned}&\hat{\boldsymbol{\Phi}}=c_{02}\{\theta\sin\theta,\theta\cos\theta,0\}\\&\big(\text{or in Cartesian coordinates }\hat{\boldsymbol{\Phi}}=c_{02}\{0,\arctan\tfrac{y}{x},0\}\big)\end{aligned} \tag{40}$$

where c_{02} is unknown constant.

This term $\hat{\boldsymbol{\Phi}}$ does not arise in the complete series (23), however it can be added as an additional particular solution that obey the vector Laplace equation. Without addition of this particular solution $\hat{\boldsymbol{\Phi}}$ one should use the full infinite series in (23) that is not useful and rather complicated. It can be checked then that the relations between the coefficients in the Flamant problem solution (39), and non-zero coefficients in the representation of the Papkovich–Neuber potential (23), (40) are the following:

$$\begin{aligned}&c_{02}=\frac{2C_1(\lambda+2\mu)}{\lambda+3\mu},\quad c_{50}=\frac{2C_3(\lambda+2\mu)}{\lambda+3\mu},\\&c_{70}=\frac{2(\lambda+2\mu)(C_3(\lambda+\mu)-C_2(\lambda+3\mu))}{(\lambda+3\mu)^2}\end{aligned} \tag{41}$$

Thus, in classical elasticity one can use the Papkovich–Neuber displacement solution to solve the Flamant problem. In the next two subsections we will provide a variant of generalization of this classical solution (39) onto the gradient elasticity. Instead of force we will prescribe the tip displacement that will simplify our analytical derivations.

3.1. Analysis of the displacement solution around the wedge apex

Using Papkovich–Neuber representation (22) we can define the solution for SGET equilibrium equations in the considered problem as

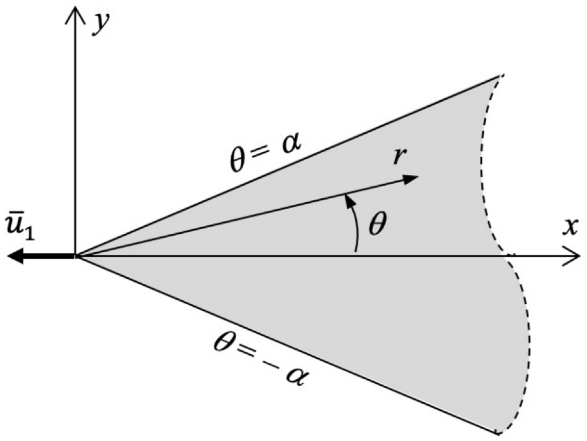

Fig. 1. Elastic wedge loaded at the apex by the tip displacement.

follows:

$$u_r = (1-\kappa)\Phi_r - r\kappa\frac{\partial \Phi_r}{\partial r} + \frac{l_2^2}{r}\frac{\partial^2 \chi}{\partial \theta^2} + l_1^2\frac{\partial \psi}{\partial r} + \hat{u}_r,$$
$$u_\theta = \Phi_\theta - \kappa\frac{\partial \Phi_r}{\partial \theta} - l_2^2\frac{\partial^2 \chi}{\partial r \partial \theta} + \frac{l_1^2}{r}\frac{\partial \psi}{\partial \theta} + \hat{u}_\theta \tag{42}$$

where we introduce an additional part of the displacement solution $\hat{\mathbf{u}} = \{\hat{u}_r, \hat{u}_\theta, 0\}$ that arises in SGET due to presence of the corresponding classical part of the solution related to $\hat{\boldsymbol{\Phi}}$ (40).

All Papkovich–Neuber potentials in (42) can be defined in a simplified form taking into account the symmetry of the problem. Namely, using standard trigonometric relations and redefining the constants, from (23) we obtain the following representation for the components of the classical vector potential $\boldsymbol{\Phi}$:

$$\Phi_r = c_{02}\theta\sin\theta + c_{50}\ln r\cos\theta + c_{70}\cos\theta + \sum_{n=1}^{\infty}\Big((r^{-n}c_{2n} + r^n c_{4n})\cos(n-1)\theta + (r^{-n}c_{5n} + r^n c_{7n})\cos(n+1)\theta\Big),$$
$$\Phi_\theta = c_{02}\theta\cos\theta - c_{50}\ln r\sin\theta - c_{70}\sin\theta + \sum_{n=1}^{\infty}\Big((r^{-n}c_{2n} + r^n c_{4n})\sin(n-1)\theta - (r^{-n}c_{5n} + r^n c_{7n})\sin(n+1)\theta\Big) \tag{43}$$

where we use all terms that arise in the classical elasticity solution (including additional potential $\hat{\boldsymbol{\Phi}}$ (40)) and also add the series with the all other terms from the complete representation of $\boldsymbol{\Phi}$ (23).

Scalar gradient potentials ϕ and χ (26) for the symmetric loading become to:

$$\psi = \sum_{n=0}^{\infty}\left(K_n\left(\frac{r}{l_1}\right)b_{1n} + I_n\left(\frac{r}{l_1}\right)b_{3n}\right)\cos n\theta,$$
$$\chi = \sum_{n=0}^{\infty}\left(K_n\left(\frac{r}{l_2}\right)d_{1n} + I_n\left(\frac{r}{l_2}\right)d_{3n}\right)\cos n\theta \tag{44}$$

Additional solution $\hat{\mathbf{u}}$ in (42) is defined heuristically. Namely, we suppose that this part of the displacement field should have the similar behavior with the classical one defined by $\hat{\boldsymbol{\Phi}}$ (40). It should be (a) bounded at the origin of the coordinates, (b) related to the $\arctan(y/x)$ function in the Cartesian coordinates, and (c) it should have the irrotational and the rotational parts both. Therefore, $\hat{\mathbf{u}}$ can be defined by using the following particular solutions for the vector Helmholtz equation that meets our requirements for the case of the symmetric loading:

$$\hat{\boldsymbol{\Psi}}_i = b_i\left\{\theta I_0\left(\tfrac{r}{l_i}\right)\sin\theta, \theta I_0\left(\tfrac{r}{l_i}\right)\cos\theta, 0\right\} : \quad \hat{\boldsymbol{\Psi}}_i - l_i^2\nabla^2 \upsilon \hat{\boldsymbol{\Psi}}_i = 0, \qquad (i = 1,2), \tag{45}$$

where b_i are some unknown constants, I_0 is zero order modified Bessel functions of the first kind (it is unbounded at infinity, however, we will consider the solution only around the wedge apex), and the values of the length scale parameters l_i should be chosen accordingly to the part of the displacement field that we need to define. Namely, since (45) contains the irrotational and the rotational parts both it is necessary to use the general Papkovich–Neuber representation to define the corresponding part of the displacement solution as follows:

$$\hat{\mathbf{u}} = l_1^2\nabla\nabla\cdot\hat{\boldsymbol{\Psi}}_1 + \hat{\boldsymbol{\Psi}}_2 - l_2^2\nabla\nabla\cdot\hat{\boldsymbol{\Psi}}_2 \tag{46}$$

This representation (46) is similar to the initial one provided by Eqs. (10) for the gradient part of the displacement field $\mathbf{u}^{(g)}$. In this representation we extract the purely potential part of $\hat{\boldsymbol{\Psi}}_1$ and purely rotational part of $\hat{\boldsymbol{\Psi}}_2$. Analog for the scalar potential ψ is obtained in (46) through the divergence of $\hat{\boldsymbol{\Psi}}_1$ (similar form of solution in SGET have been used, e.g. in Lurie et al. (2011)). Component representation for (46) can be easily obtained via standard definitions of vector operators and we do not present it here for clarity.

Now, let us consider the 2π-periodic part of solution (42)–(44) together with particular solutions defined by Eq. (40), (46). These part includes the classical singular logarithmic terms and has the following form:

$$\begin{aligned}
(u_r)_{2\pi} = {} & \Big(c_{02}(1-\kappa) + b_1\big(I_0(\tfrac{r}{l_1}) - \frac{l_1}{r}I_1(\tfrac{r}{l_1})\big) + b_2\frac{l_2}{r}I_1(\tfrac{r}{l_2})\Big)\theta\sin\theta \\
& + \Big(c_{70}(1-\kappa) - c_{50}\kappa + c_{50}(1-\kappa)\ln r + (1+\kappa)r^{-2}c_{22} + (1-3\kappa)r^2 c_{42} \\
& + b_1\big(\frac{l_1}{r}I_1(\tfrac{r}{l_1}) - \frac{l_1^2}{r^2}I_0(\tfrac{r}{l_1})\big) - b_2\big(\frac{l_2}{r}I_1(\tfrac{r}{l_2}) - \frac{l_2^2}{r^2}I_0(\tfrac{r}{l_2})\big) \\
& + \frac{l_2^2}{r}K_1(\tfrac{r}{l_2})d_{11} + \frac{l_2^2}{r}I_1(\tfrac{r}{l_2})d_{31} - \frac{l_1}{2}\Big(K_0(\tfrac{r}{l_1}) + K_2(\tfrac{r}{l_1})\Big)b_{11} \\
& + \frac{l_1}{2}\Big(I_0(\tfrac{r}{l_1}) + I_2(\tfrac{r}{l_1})\Big)b_{31}\Big)\cos\theta \\
(u_\theta)_{2\pi} = {} & \Big(c_{02}(1-\kappa) + b_1\frac{l_1}{r}I_1(\tfrac{r}{l_1}) + b_2\big(I_0(\tfrac{r}{l_2}) - \frac{l_2}{r}I_1(\tfrac{r}{l_2})\big)\Big)\theta\cos\theta \\
& + \Big(-c_{02}\kappa - c_{70}(1-\kappa) - c_{50}(1-\kappa)\ln r \\
& + (1+\kappa)r^{-2}c_{22} + (1+\kappa)r^2 c_{42} \\
& + b_1\big(\frac{l_1}{r}I_1(\tfrac{r}{l_1}) - \frac{l_1^2}{r^2}I_0(\tfrac{r}{l_1})\big) - b_2\big(\frac{l_2}{r}I_1(\tfrac{r}{l_2}) - \frac{l_2^2}{r^2}I_0(\tfrac{r}{l_2})\big) \\
& + \frac{l_2}{2}\Big(K_0(\tfrac{r}{l_2}) + K_2(\tfrac{r}{l_2})\Big)d_{11} - \frac{l_2}{2}\Big(I_0(\tfrac{r}{l_2}) + I_2(\tfrac{r}{l_2})\Big)d_{31} \\
& - \frac{l_1^2}{r}K_1(\tfrac{r}{l_1})b_{11} - \frac{l_1^2}{r}I_1(\tfrac{r}{l_1})b_{31}\Big)\sin\theta
\end{aligned} \tag{47}$$

Satisfaction of equilibrium equations of SGET (9) by this solution (47) will be provided automatically since we use the Papkovich–Neuber representation (it can be also checked by the direct substitution).

Assessment for the behavior of the displacement field $\mathbf{u}_{2\pi} = \{(u_r)_{2\pi}, (u_\theta)_{2\pi}, 0\}$ around the wedge apex can be obtained by evaluation of the limits for the small values of the radial coordinate (namely, for the small r/l_1 and r/l_2 ratios). From (47) we find:

$$\begin{aligned}\lim_{r\to 0}(u_r)_{2\pi} &= \Big((c_{50}(1-\kappa)+\frac{l_2 d_{11}+l_1 b_{11}}{2})\ln r \\ &+ ((1+\kappa)c_{22} - l_1^2(b_{11}l_1+b_1)+l_2^2(d_{11}l_2+b_2))r^{-2}+O(1)\Big)\cos\theta \\ \lim_{r\to 0}(u_\theta)_{2\pi} &= \Big(-(c_{50}(1-\kappa)+\frac{l_2 d_{11}+l_1 b_{11}}{2})\ln r \\ &+ ((1+\kappa)c_{22} - l_1^2(b_{11}l_1+b_1)+l_2^2(d_{11}l_2+b_2))r^{-2}+O(1)\Big)\sin\theta\end{aligned} \tag{48}$$

Important result here is that these limits will have the finite values if the solution of the problem allows the following relations between the constants:

$$c_{50} = -\frac{l_2 d_{11}+l_1 b_{11}}{2(1-\kappa)}, \qquad c_{22} = \frac{l_1^2(b_{11}l_1+b_1)-l_2^2(d_{11}l_2+b_2)}{1+\kappa} \tag{49}$$

In this case the classical logarithmic singularity and the additional gradient term r^{-2} will be vanished in (48) and the displacement field around the wedge apex will be regular.

Further, we can found the infinitesimal dilatation and infinitesimal rotation vector related to $\mathbf{u}_{2\pi}$. Of interest, are the limits of these quantities around the wedge apex. From (47) taking into account (49) one can found that these limits are the following:

$$\begin{aligned}\lim_{r\to 0}\Theta_{2\pi} &= \frac{1}{2(1-\kappa)}\Big(c_{02}(2-6\kappa+4\kappa^2)+2b_1(1-\kappa) \\ &+ b_{11}l_1 - d_{11}l_2(1-2\kappa)\Big)r^{-1}\cos\theta + O(r) \\ \lim_{r\to 0}\boldsymbol{w}_{2\pi} &= \Big\{0, 0, \frac{1}{4(1-\kappa)}\Big(2c_{02}(1-\kappa)+2b_2(1-\kappa) \\ &- b_{11}l_1 + d_{11}l_2(1-2\kappa)\Big)r^{-1}\sin\theta + O(r)\Big\}\end{aligned} \tag{50}$$

It is seen, that the bounded solution for the dilatation and rotation at $r = 0$ can be obtained assuming the following relations between the constants:

$$\begin{aligned}b_1 &= \frac{c_{02}(2-6\kappa+4\kappa^2)+b_{11}l_1 - d_{11}l_2(1-2\kappa)}{2(\kappa-1)}, \\ b_2 &= \frac{2c_{02}(1-\kappa)-b_{11}l_1+d_{11}l_2(1-2\kappa)}{2(\kappa-1)}\end{aligned} \tag{51}$$

It can be shown then that the strain field $\varepsilon_{ij} = (u_{i,j}+u_{j,i})/2$ and the Cauchy stresses τ_{ij} (7) will be also bounded at the wedge apex if one use the relations between the constants (49) and (51). Moreover, the singularity-free solution for the traction components at the wedge faces $\theta = \pm\alpha$ can be also evaluated in this case. Since the general constitutive equations for the double stresses and for tractions are rather complicated it is useful to provide such derivations within the simplified theory. At first, we will use SSGET (Section 2.5). Within SSGET the solution and the derivations are all the same as presented in (47)–(51). The only difference with the general theory will be that in SSGET one should use the single value of the length scale parameter $l = l_1 = l_2$ in (47)–(51).

Definitions for the surface traction components $\boldsymbol{t}$ (4) at the wedge faces $\theta = \pm\alpha$ in polar coordinates within SGET are given by:

$$t_r = \tau_{r\theta} - \frac{\partial \mu_{rr\theta}}{\partial r} - \frac{\partial \mu_{r\theta r}}{\partial r} - \frac{1}{r}\left(\mu_{rr\theta}+\mu_{r\theta r}-\mu_{\theta\theta\theta}+\frac{\partial \mu_{r\theta\theta}}{\partial\theta}\right) \tag{52}$$

$$t_\theta = \tau_{\theta\theta} - \frac{\partial \mu_{\theta r\theta}}{\partial r} - \frac{\partial \mu_{\theta\theta r}}{\partial r} - \frac{1}{r}\left(\mu_{r\theta\theta}+\mu_{\theta r\theta}+\mu_{\theta\theta r}+\frac{\partial \mu_{\theta\theta\theta}}{\partial\theta}\right) \tag{53}$$

where we take into account that the wedge faces are flat and its mean curvature equals to zero $H = 0$.

Evaluating the strain and strain gradients for the displacement solution (47) and using then the constitutive assumptions of SSGET to define the double stress components μ_{ijk} according to (28) and using standard Hook's low for the Cauchy stresses τ_{ij} (7) after long algebraic derivations one can find that around the wedge apex the traction components at the boundaries $\theta = \pm\alpha$ (52), (53) can be presented as follows:

$$\begin{aligned}\lim_{r\to 0}(t_r)_{2\pi} &= \frac{1}{4(1-\kappa)}\Big(4c_{02}(1-\kappa)\mu + b_{11}l(2(1-\kappa)\lambda+(3-5\kappa)\mu) \\ &+ d_{11}l(1-3\kappa)\mu\Big)r^{-1}\sin\alpha + O(r)\end{aligned} \tag{54}$$

$$\begin{aligned}\lim_{r\to 0}(t_\theta)_{2\pi} &= \frac{1}{4(1-\kappa)}\Big(4c_{02}(1-\kappa)(1-2\kappa)(\lambda+2\mu) \\ &- (b_{11}+d_{11})l(2(1-2\kappa)\lambda+(1-5\kappa)\mu)\Big)r^{-1}\cos\alpha + O(r)\end{aligned} \tag{55}$$

From (54), (55) we obtain two more conditions for the constants that will provide us the bounded values of tractions at the wedge faces around $r = 0$:

$$\begin{aligned}b_{11} &= \frac{6c_{02}(\kappa-1)\mu((1-2\kappa)\lambda+(1-4\kappa)\mu)}{l(\lambda+\mu)(2(1-2\kappa)\lambda+(1-5\kappa)\mu)}, \\ d_{11} &= \frac{2c_{02}(1-\kappa)((2-4\kappa)\lambda^2+9(1-2\kappa)\lambda\mu+(7-20\kappa)\mu^2)}{l(\lambda+\mu)(2(1-2\kappa)\lambda+(1-5\kappa)\mu)}\end{aligned} \tag{56}$$

Thus, at this stage we obtain 6 conditions (49), (51), (56) for 7 constants c_{02}, c_{50}, c_{22}, b_1, b_2, b_{11}, d_{11}. Satisfaction of these conditions provide us a regular solution at least for the displacement field, strain, Cauchy stress and tractions (at $\theta = \pm\alpha$) around the wedge apex. These conditions are independent and we can use them to define 6 constants through the last one that will remain unknown. For example, such unknown constant can be c_{02}. In this case all other constants can be found from (49), (51), (56) and their representation within SSGET will be the following:

$$\begin{aligned}&c_{22} = \frac{6l^2(\lambda+\mu)(\lambda+3\mu)}{(\mu-\lambda)(3\lambda+5\mu)}c_{02}, \quad c_{50} = \frac{4(\lambda+2\mu)}{\mu-\lambda}c_{02}, \quad b_1 = \frac{3\mu(\lambda+3\mu)}{(\lambda-\mu)(\lambda+2\mu)}c_{02}, \\ &b_2 = \frac{\lambda+3\mu}{\mu-\lambda}c_{02}, \quad b_{11} = 0, \quad d_{11} = \frac{4(\lambda+3\mu)}{\lambda-\mu}c_{02}\end{aligned} \tag{57}$$

where we take into account that $\kappa = \frac{\lambda+\mu}{2(\lambda+2\mu)}$.

Remaining constant c_{02} should be found from the external loading conditions and an example of such solution will be presented in the next subsection. Note, that presented result is obtained within SSGET, which contains two length scale parameters in equilibrium equations $l_1 = l_2 = l$. For this particular case of the strain gradient elasticity we obtain that b_{11} should be equal to zero in (57). Nevertheless, the potential part of the gradient part of displacements in this solution will be non-zero since, e.g. constant b_1 has non-zero values and it defines the particular solution $\hat{\mathbf{u}}$ (45), (46), with non-zero dilatation.

Now it is important to evaluate the solution structure within the simplified theories, which do not contain the gradient part of dilatation or the rotation and do not provide the regularization for the corresponding parts of the solution. Consider at first DGET (Section 2.6). In this theory the second length scale parameter equals to zero ($l_2 = 0$, $l_1 = l$) and the gradient part of the displacement field should be irrotational (33). This means that potentials χ in (42), (44) and $\hat{\boldsymbol{\Psi}}_2$ in (46) should be avoided by using zero values of the corresponding coefficients, i.e. we should use $d_{11} = 0$ and $b_2 = 0$ in (47). Therefore, in this theory we will have only 5 constants c_{02}, c_{50}, c_{22}, b_1, b_{11} and 6 conditions (49), (51), (56) that should be fulfilled to provide the singularity-free solution. In DGET the conditions for the bounded displacement field at the wedge apex instead of (49) will be:

$$c_{50} = -\frac{l_1 b_{11}}{2(1-\kappa)}, \qquad c_{22} = \frac{l^2(b_{11}l+b_1)}{1+\kappa} \tag{58}$$

For the bounded dilatation and rotation instead of (51) we will obtain:

$$b_1 = \frac{c_{02}(2-6\kappa+4\kappa^2)+b_{11}l}{2(\kappa-1)}, \qquad c_{02} = \frac{b_{11}l}{2(1-\kappa)} \tag{59}$$

Conditions for non-singular tractions (52), (53) after application of DGET constitutive assumptions (31) will provide us:

$$b_{11} = 0, \qquad c_{02} = \frac{b_{11} l}{2(1-\kappa)} \tag{60}$$

(the second condition coincides here with those one in (59)).

It is seen now, that relations (58)–(60) can be fulfilled only by the trivial solution for the all constants, such that no classical terms will arise in the displacement field and no external loading can be prescribed at the wedge apex. From this result we can conclude that the considered type of the boundary value problem within DGET will always contain singularities and its solution will violates some of these conditions (58)–(60).

Next, let us consider CST (Section 2.7). In this theory the first length scale parameter equals to zero ($l_1 = 0$, $l_2 = l$) and we should use the purely rotational gradient part of the displacement solution (37). Therefore, potentials ψ in (42), (44) and $\hat{\boldsymbol{\Psi}}_1$ in (46) should be avoided such that we should use $b_{11} = 0$ and $b_1 = 0$ in (47). Thus, in CST we have only 5 available constants (c_{02}, c_{50}, c_{22}, b_2, d_{11}) for 6 conditions (49), (51), (56), which can be derived in the following form:

- for bounded displacements instead of (49):

$$c_{50} = -\frac{l d_{11}}{2(1-\kappa)}, \qquad c_{22} = \frac{-l^2(d_{11} l_2 + b_2)}{1+\kappa} \tag{61}$$

- for bounded dilatation and rotation instead of (51):

$$c_{02} = \frac{d_{11} l (1-2\kappa)}{(2-6\kappa+4\kappa^2)}, \quad b_2 = \frac{2c_{02}(1-\kappa) + d_{11} l (1-2\kappa)}{2(\kappa-1)} \tag{62}$$

- and taking into account constitutive relations (35) conditions for the bounded tractions at wedge faces in CST instead of (56) will become to:

$$d_{11} = 0, \qquad c_{02} = 0 \tag{63}$$

Thus, in CST we also found that only the trivial solution for the constants may provide the regularization of the field variables. Therefore, for the considered problem, CST solution cannot be developed without singularities and some of relations (61)–(63) will be violated.

From the presented derivations it is seen that the bounded solutions for the generalized Flamant problem can be obtained only within those gradient theories that have two non-zero length scale parameters in the equilibrium equations. Such theories are, for example, the general Mindlin–Toupin SGET or SSGET. Simplified theories like DGET and CST do not provide the regular solutions and will contain unavoidable singular terms. Generally, it seems that the edge-type loading in DGET and CST will always lead to the non-physical singular solutions.

Note, that in the presented solution (47) we used only 2π-periodic terms from series Eq. (43), Eq. (44). However, it can be shown that all other terms that persist in the Papakovich–Neuber solution and that are unbounded at $r = 0$ (terms with high order Bessel functions $K_n(\frac{r}{l})$ and with radial functions r^{-n}) should not be included into solution because they contain unavoidable singularities. Thus, the trivial zero values for the coefficients that stay before these terms in series representation of the Papkovich–Neuber solution should be used. Non-singular high-order terms (with $I_n(\frac{r}{l})$ and r^n functions) will arise in the solution if one consider not the asymptotic analysis around the wedge apex but the far field solutions. However, it seems, that the closed form or the series solution for such problem may not be available. Such problems will be better to solve by using discretization of the domain with numerical finite element or boundary element methods. Examples of such FE solutions will be presented in the next section.

In the presented analysis we also did not provide an explicit assessments for the strain gradients, double stresses and components of traction at surfaces $r = const$. This is due to the fact that presented solution (47) does not have enough constants to avoid the singularities in these fields. Moreover, the singular solutions for traction at the surfaces with normals along radial direction has a clear physical meaning. Singularities in these quantities cannot be avoided since in the considered problem we have a concentrated force applied at the infinitesimally small area, i.e. at the wedge apex. Nevertheless, as it is shown above in the definitions of traction components at the wedge faces $\theta = const$ the singular terms are canceled. This is some kind of a lucky case for the presented solution. Similar situation arise for the crack problems in SGET, where surface tractions and double tractions are singular, while the strains and the Cauchy stresses are bounded (Gourgiotis and Georgiadis, 2009; Sciarra and Vidoli, 2013).

Thus, based on the representation of the displacements given by Eqs. (47) we can obtain a closed form solutions (around the wedge apex) if we can avoid using the double stresses and related double tractions (see (4)) in the boundary conditions. This can be done for the case of the essential high-order boundary conditions prescribed at the wedge faces. In the boundary value problem formulation of SGET (3) on the body boundaries one can define the gradient of displacement instead of double traction. This variant of the problem can be explicitly solved by using presented approach (see next subsection). Solutions for the natural high-order boundary conditions will be provided numerically in Section 4.

3.2. Asymptotic solution for the wedge with stiffened boundaries

Let us provide an example of analytical solution within SSGET for the following formulation of the boundary value problem for the wedge-type domain (see Fig. 1):

$$\begin{cases} \theta \in [-\alpha, \alpha]: & \nabla \cdot \boldsymbol{\sigma} = 0 \\ \theta = \pm\alpha: & \boldsymbol{t} = 0 \quad i.e. \quad t_r = 0, \quad t_\theta = 0, \\ & \partial_n \mathbf{u} = 0 \quad i.e. \quad \partial_n u_r = \frac{1}{r}\frac{\partial u_r}{\partial \theta} - \frac{u_\theta}{r} = 0, \quad \partial_n u_\theta = \frac{u_r}{r} + \frac{1}{r}\frac{\partial u_\theta}{\partial \theta} = 0, \\ r = 0 \ (apex): & \mathbf{u} = \bar{\mathbf{u}}_e, \quad i.e. \quad u_r = -\bar{u}_1 \cos\theta, \quad u_\theta = \bar{u}_1 \sin\theta \end{cases} \tag{64}$$

Here we assume that the wedge is loaded by the tip displacement prescribed in horizontal direction (in Cartesian coordinates it will be $\bar{\mathbf{u}}_e = \{-\bar{u}_1, 0, 0\}$). Wedge boundaries are free from the surface tractions. However, the additional high-order boundary conditions are prescribed with respect to the normal gradients of displacements. Thus, the wedge does not have fully stress-free state at the surfaces, but on its faces we use the conditions that restricted its deformations. This is why we called this problem as the wedge with stiffened boundaries. Uniqueness for such kind of the problems with mixed-type boundary conditions in SGET have been proved recently in Nazarenko et al. (2021).

At the remote distance from the tip (at some surface $r = r_0$) we assume that there exist some appropriate external loading that provides a global equilibrium of a wedge such that the boundary conditions at this remote surface will be out of consideration.

The following analysis will be restricted for the small area around the apex ($r \to 0$) since the full-field solution of the considered problem cannot be found analytically within SGET in a closed form via proposed approach. Using series representation (22)–(26) one will meet the problem of satisfaction of the boundary conditions along the wedge faces because the classical and the gradient terms in general solution differently depends on radial coordinate ($r^{\pm n}$ in classical part and modified Bessel functions in gradient part). Application of some integral transforms will also leads to the problems. For example, application of the Mellin transform (that is usually involved in classical wedge problems) for the SGET statement leads to some delay differential equations, which closed form solutions are also not available. Hence, it is convenient to find the full-field solutions numerically (see next section).

For the analysis around the wedge apex we can use the solution (47), hich provids that the equilibrium equations of SSGET are fulfilled. We may not include the high order bounded terms into this solution,

since they will rapidly decay with $r \to 0$. High order singular terms should be neglected as it was mentioned above. Using the derived relations for the constants (57) in the solution (47) we will also avoid the singularities in the displacement field and at the same time we will provide that around the wedge apex the tractions (52), (53) and the strain field (and also the gradient of displacements) will be bounded. Moreover, it can be checked that relations (57) provide us that around the wedge apex the displacement gradients and the surface tractions (52), (53) will depend on the radial coordinate as $O(r)$. Therefore, for the small values of r our solution (47), (57) identically satisfy the required boundary conditions for tractions $t_r \equiv 0$, $t_\theta \equiv 0$ (similarly to classical elasticity) and also for the normal gradient of displacements $\partial_n u_r \equiv 0$, $\partial_n u_\theta \equiv 0$.

Physical meaning for the vanishing of the displacement gradients at $r \to 0$ is that the wedge apex in the presented asymptotic SGET solution behaves like a rigid body. This is a natural consequence of the fact that the apparent stiffness of the smaller bodies in SGET becomes higher. Moreover, at the wedge apex we have two closed boundaries with prescribed stiffened constrains and their influence extended on the whole (small) volume around the apex.

The remaining task is to define the tip displacement and to find the corresponding values of the constants that were not already defined. Substituting (57) into (47) and evaluating the limit, one can find the following solution for the displacements of the wedge apex (at $r = 0$):

$$\lim_{r\to 0} \mathbf{u} = \{U\cos\theta, -U\sin\theta, 0\} + O(r) \tag{65}$$

where we introduce the following notations:

$$\begin{aligned} U &= c_{02}S(l) + \tfrac{(b_{31}+d_{31})}{2} l + c_{70}(1-\kappa) \\ S(l) &= \tfrac{(5+8\gamma)\lambda^2+4(3+10\gamma)\lambda\mu+(7+48\gamma)\mu^2}{4(\lambda-\mu)(\lambda+2\mu)} - \tfrac{2(\lambda+3\mu)}{(\lambda-\mu)}\log(2l) \end{aligned} \tag{66}$$

and $\gamma \approx 0.5772$ is Euler's constant.

Then, we can use the boundary condition for the displacements at the wedge apex assuming that $\lim_{r\to 0}\mathbf{u} = \bar{\mathbf{u}}_e$ (see (64)). In such a way we found:

$$U = -\bar{u}_1 \quad \Rightarrow \quad c_{02} = -\frac{2\bar{u}_1 + (b_{31}+d_{31})l + 2c_{70}(1-\kappa)}{2S(l)} \tag{67}$$

Thus, we obtain one more relation for the constants that persist in our solution. Here we used this relation to define c_{02}. All other constants $b_{31}, d_{31}, c_{70}, c_{42}$ in (47) remain unknown and they should be defined from the boundary conditions at the remote distance from the wedge tip. Dependence of the solution on the value of the wedge angle α will also arise from the satisfaction of these boundary conditions (similarly to classical elasticity solution (39)). It can be also found that the traction components at the surfaces with normals along the radial coordinates ($r = const$, $\mathbf{n} = \{1,0,0\}$) behaves as $\sim r^{-1}\log r$ around the origin of coordinates in the presented solution. This singularity can be treated as the consequence of an applied loading at an infinitely small area at tip end of the sharp edge.

4. Numerical simulations for the finite size wedge

Our analytical derivations for the small area around the wedge apex are supported by the full-field numerical solutions for the finite size wedges. Numerical simulations were performed by using the mixed FEM formulation of SGET implemented in the Weak Form PDE interface in Comsol. These implementation bases on the introduction of extra independent variables for strains and it was described in details elsewhere (Reiher et al., 2017; Andreaus et al., 2016; Giorgio, 2016; Giorgio et al., 2018b). In simulations we used the third order Hermite polynomials as the shape functions for the kinematical variables and for the Lagrange multipliers inside the domain. The second order Lagrange polynomials were used for definition of the essential boundary conditions. Triangular mesh elements and standard Comsol direct solver (MUMPS) were used to find numerical solutions.

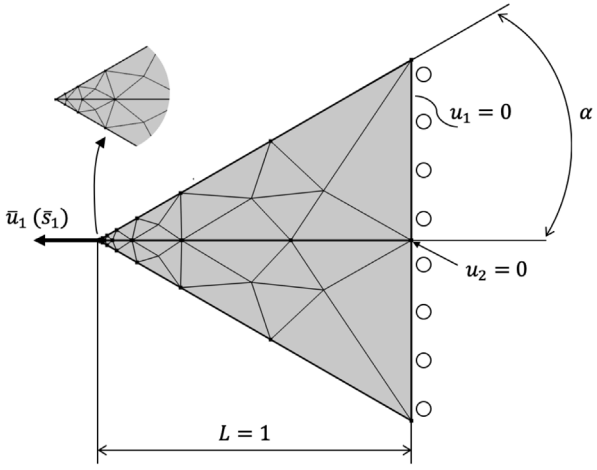

Fig. 2. FE model of the wedge used in numerical simulations.

As an example, we consider a very simple but representative problem for the triangular body with applied tensile loading at one apex and constrained at the opposite edge (Fig. 2). Length of the domain is denoted as L and its opening angle is 2α. The out-of-plane size of the domain is assumed to be $D = L$. In FE simulations we prescribed the tip displacement $\bar{u}_1$ (or the edge force $\bar{s}_1$) and evaluated the realized Cauchy stresses τ_{ij} (or the displacement u_1) at the wedge apex for different size h of the finite element mesh. The stress-free boundary conditions for tractions and double tractions are prescribed for the upper and lower faces of the wedge. Considered boundary value problem is the following:

$$\begin{cases} \theta \in [-\alpha,\alpha]: & \nabla\cdot\boldsymbol{\sigma} = 0 \\ \theta = \pm\alpha: & \boldsymbol{t} = 0, \quad \boldsymbol{m} = 0 \\ r = 0\ (apex): & \mathbf{u} = \{-\bar{u}_1, 0, 0\}, \quad (or\ \ \boldsymbol{s} = \{-\bar{s}_1, 0, 0\}) \end{cases} \tag{68}$$

For this problem we found FE solutions within different simplified gradient theories using Comsol. Reducing the mesh size around the wedge apex we provide an assessments on the convergence of the solution for the mentioned above field variables (τ_{ij} for prescribed tip displacement or u_1 for prescribed edge traction). Solutions are given for the element sizes from $h = L$ (single element for the whole wedge) down to $h = 10^{-4}L$.

In the simulations we considered the wedge with different opening angles within the models with constitutive assumptions of SSGET, DGET and CST. Length scale parameter l is varied in the range $l = [10^{-3}L, L]$. Parameter η in CST (see (34)) does not make a qualitative impact and for the presented plots we used $\eta = 0.5$. Material Young's modulus is set to be $E = 1$ GPa and Poisson's ratio is $\nu = 0.3$. Prescribed displacement value equals to $\bar{u}_1 = 0.01L$. Prescribed edge force is defined by relation $\bar{s}_1 = 0.01EH$, where $H = 2L\tan\alpha$ is the height of the edge that is opposite to the loaded apex. Such definition of $\bar{s}_1$ provide us the same levels of mean stress τ_{11} in the cross sections of the wedges with different opening angles. Normalized values of stresses that will be presented in the following plots are evaluated as $\hat{\tau}_{ij} = \tau_{ij}L/(\bar{u}_1 E)$ (for prescribed $\bar{u}_1$). Normalized displacements are evaluated as $\hat{u}_1 = u_1 EH/(\bar{s}_1 L)$ (for prescribed $\bar{s}_1$).

Examples of the deformed state of the wedge that is realized for the prescribed tip displacement within different gradient theories is shown in Fig. 3. All these results are given for the finest mesh used in the simulations ($h = 10^{-4}L$) and for the opening angle $2\alpha = \pi/3$. Length scale parameter is $l = 0.1L$. It is seen that in SSGET (Fig. 3a) the deformations of the wedge are smooth and the stress concentration is not very high. Non-uniform stress state realizes in almost the whole domain. In opposite, in DGET and in CST (Fig. 3b, c) we found that the

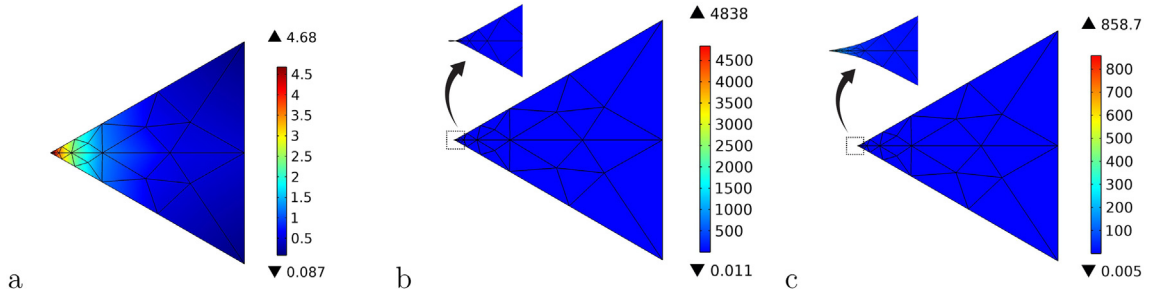

Fig. 3. Examples of the deformed state of the wedge under prescribed tip displacement and distribution of the normalized Cauchy stresses $\hat{\tau}_{11}$ in SSGET (a) in DGET (b) and in CST (c) solutions.

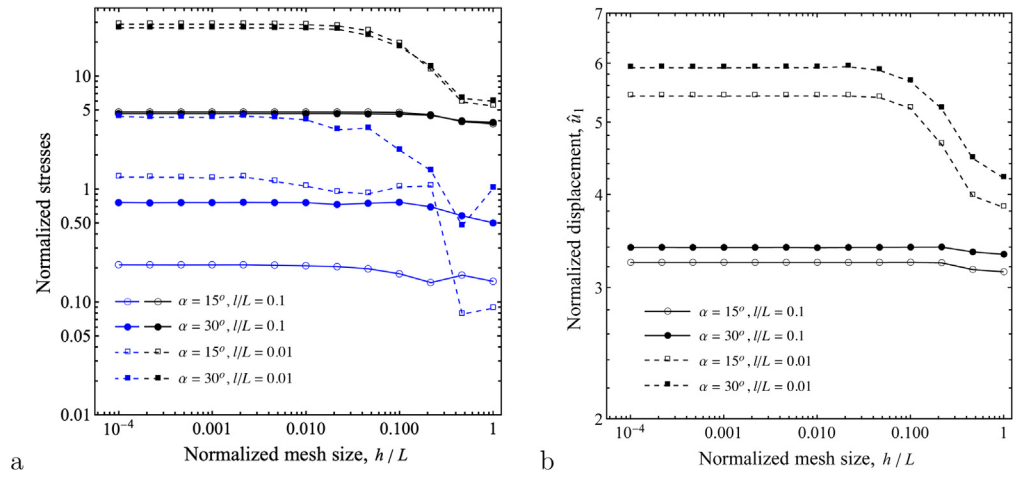

Fig. 4. Dependence of SSGET numerical solutions on the mesh size, a: Normalized stresses $\hat{\tau}_{11}$ (black lines) and $|\hat{\tau}_{22}|$ (blue lines) at the wedge apex loaded by the prescribed tip displacement, b: Normalized displacement at the wedge apex loaded by the edge force.

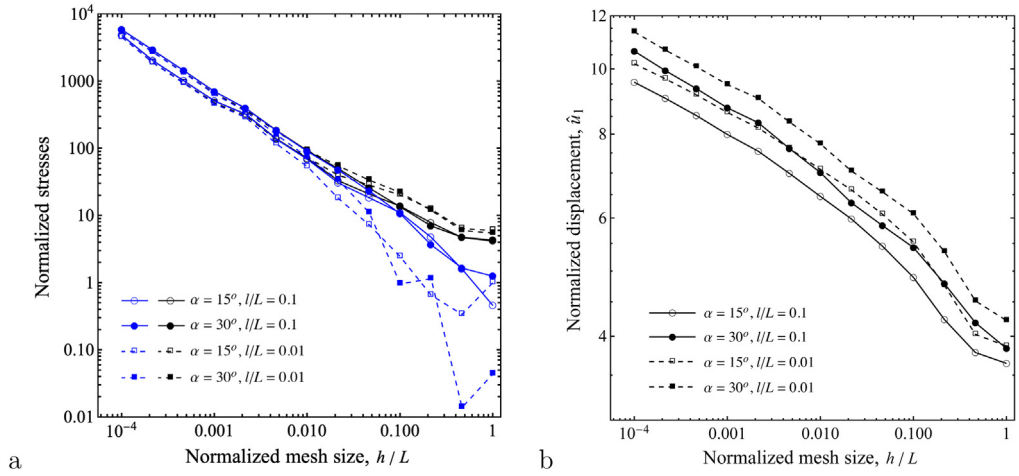

Fig. 5. Dependence of DGET numerical solutions on the mesh size, a: Normalized stresses $\hat{\tau}_{11}$ (black lines) and $|\hat{\tau}_{22}|$ (blue lines) at the wedge apex loaded by the prescribed tip displacement, b: Normalized displacement at the wedge apex loaded by the edge force.

deformations are strongly localized around the loaded apex and that the stress concentration becomes in several orders higher than in SSGET. Moreover, in DGET solution (Fig. 3b) there arise a strong distortion of the mesh around the apex.

Evaluation of the solutions convergence is presented in Figs. 4–6. For SSGET solution (Fig. 4) it is seen, that reducing the mesh size we obtain a stable solution for stresses and displacements. Asymptotic values achieved even for the mesh size of the order $h/L = 0.001...0.01$. Notably, that these asymptotic values of stresses and displacements increases both for the smaller length scale parameter (more classical behavior). However, for the smaller opening angles longitudinal stress τ_{11} increases, while the transverse stresses τ_{22} and displacements decrease. This can be explained by the fact that in the wedges with smaller opening angles the upper and lower faces around apex are closer to each other. Thus, the stress-free state of these faces extended into the volume, such that the state of the wedge becomes more similar to the uniaxial tension.

Convergence analysis of the numerical solutions within DGET and CST is presented in Figs. 5 and 6. For these theories both we observe the mesh depended solutions for stresses as well as for the displacements

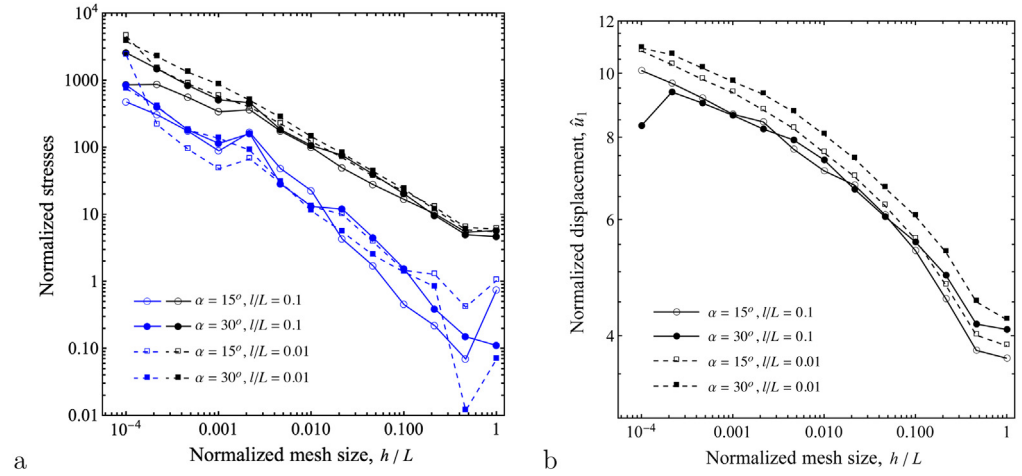

Fig. 6. Dependence of CST numerical solutions on the mesh size, a: Normalized stresses $\hat{\tau}_{11}$ (black lines) and $|\hat{\tau}_{22}|$ (blue lines) at the wedge apex loaded by the prescribed tip displacement, b: Normalized displacement at the wedge apex loaded by the edge force.

for any values of the length scale parameters and wedge opening angle. Exponential growth of stresses is observed on the presented plots (Figs. 5a, 6a). For the displacements there arise some kind of sub-exponential growth (Figs. 5b, 6b), though the behavior of the solution for the smaller mesh than $h = 10^{-4} L$ was hard to check due to rounding errors that arise in the solution.

Thus, from the presented results for the convergence of the numerical solutions it is seen that the strain gradient models with DGET or CST constitutive assumptions cannot sustain the prescribed edge forces and tip displacements. Such solutions significantly affected by the mesh size and they are meaningless for the structural analysis. In opposite to these incomplete theories, in SSGET we found the well converged and stable solutions that can be used for the assessment of the material behavior under the edge loading. Such kind of the loading may arise in the macro-scale problems with the localized forces, which is suitable to describe as the concentrated tractions due large difference between the loaded area and the whole area of the domain. Also the models with the edge-type loading can be suitable for the micro- and nano-scale simulations, for example for the analysis of the stress state around the loaded edges and sharp corners of single crystals and 2D materials during the atomic force microscopy, nano-indentation or manipulation. As it is shown analytically in the previous section and numerically in the present section, the gradient theories with dilatation and rotation effects both can be involved in the such type analysis.

For SSGET we additionally provide an analysis of stress concentration around the apex of wedges with different opening angles (Fig. 7) and different length scale parameters (Fig. 8). In Fig. 7 it is seen, that the decrease of the opening angle leads to some increase of the longitudinal stresses $\hat{\tau}_{11}$ and decrease of the transverse stresses $\hat{\tau}_{22}$. Interestingly, that for the large relative values of the length scale parameter the angular dependence of $\hat{\tau}_{11}$ becomes negligible, while $\hat{\tau}_{22}$ strongly depends on α in any case. Decrease of the length scale parameter l leads to the higher stress concentration (Fig. 8). In the limiting case $l \to 0$ SSGET reduces to the classical elasticity theory. Thus, the stresses around the loaded apex in this case become infinite and numerical solution becomes mesh-dependent.

Finally, based on Fig. 8 we can give an assessments for the relation between the absolute value of the wedge size and stress concentration. It is known that typical values of the length scale parameters of single crystals have the order of interatomic distance, i.e. within SSGET we have $l = l_1 = l_2 \approx 1$ Å (Lazar et al., 2021). Therefore, if the loading is applied at the atomically sharp edge of single crystal and provides the maximum remote tensile stress equals to $\tau_{11} = 1$ MPa at distance $L = 1000l = 100$ nm from the edge tip. Then, the predicted level of maximum stress around the tip will be of the order $\tau_{11} = 110$–150 MPa depending on the angle between faces that form the edge (see Fig. 8). Such loading may arise, for example in the experiments with indentation, when the sharp edge of the crystal is penetrated into some stiff substrate.

In the inhomogeneous materials, the values of the length scale parameters may have the order of the unit cell size or the size of the inhomogeneity. For example, in polycrystalline ceramics, the identified values of the length scale parameter typically have the order $10-60\,\mu$m (see Vasiliev et al. (2021b)). Thus, in such materials for the case $l = l_1 = l_2 \approx 10\,\mu$m the stress concentration $\hat{\tau}_{11} = 110$–150 is predicted for the wedge length $L = 10$ mm.

5. Conclusions

Main result of the present contribution is that we show that the edge type loading within the incomplete gradient elasticity theories leads to the singular solutions. In opposite to general Mindlin–Toupin SGET, edge forces cannot be used directly in the theories, which do not provide regularization for the dilatational and rotational part of the solution both. Around the sharp edge loaded by the concentrated force or the tip displacement there arise the complex stress and strain state. Rotational and dilatational field become singular both in classical elasticity. Therefore, the regularization of the solution can be provided only within the full theories that take into account the gradient effects in the dilatation and in the rotations. This result is obtained based on the analytical studies with the Papkovich–Neuber solution (which simplified form for SGET is also provided here) and numerically by using mixed FEM simulations. For the general SGET we validate explicitly its ability for regular displacement and strain field around the sharp edges, though the singularities remain in double stresses and second gradient of displacements. Further regularization of the solution can be obtained only within the high order gradient theories.

Presented results are obtained for an example of the symmetrical loading, though it can be easily extended for the anti-symmetrical one. Similar results can be found in this case for the considered gradient theories that is the task for the authors' future work. In the future it is also planned to consider the problem with re-entrant corner under concentrated loading applied at the internal edge. For such problem, one should use the extended variant of series (23), (26) with additional terms that depend on the angle of the notch (for the remotely applied loading such analysis within the Knein–Williams technique was performed in Gourgiotis and Georgiadis (2011) and Gourgiotis et al. (2010)). Also it is important to note that the regular solutions for

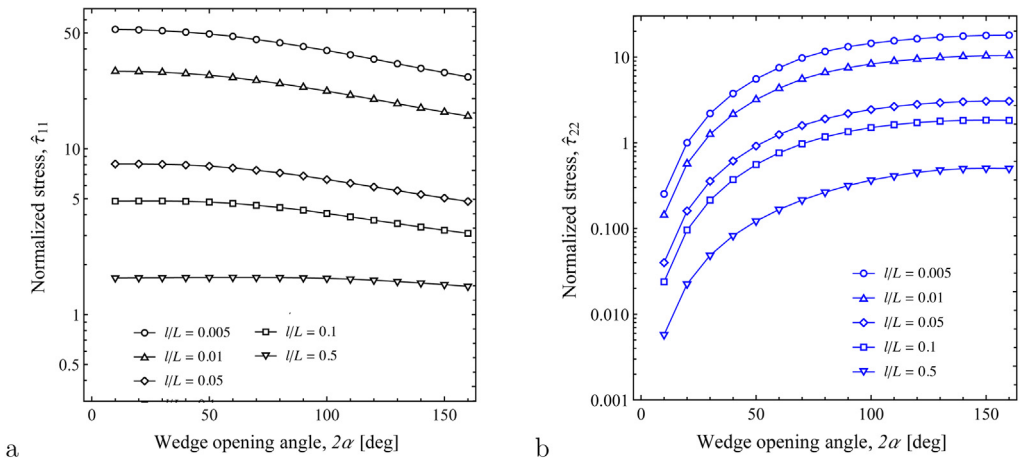

Fig. 7. Dependence of stress concentration on the wedge opening angle in SSGET numerical solutions, a: $\hat{\tau}_{11}$, b: $\hat{\tau}_{22}$.

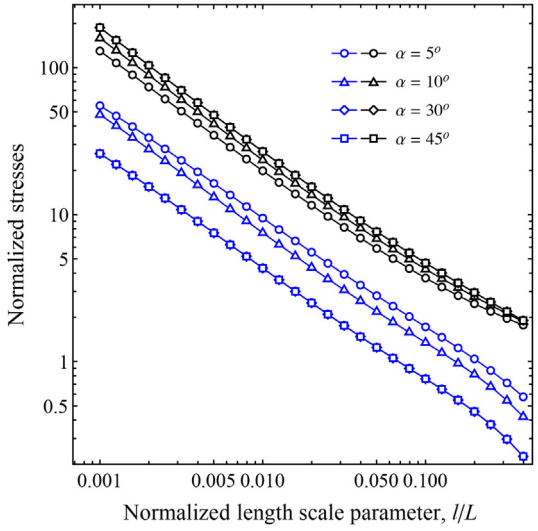

Fig. 8. Dependence of stress concentration on the length scale parameter in SSGET numerical solution ($\hat{\tau}_{11}$ – black lines, $\hat{\tau}_{22}$ – blue lines).

the edge-type loading can be also obtained within incomplete gradient theories formulated with finite strain effects (Eremeyev et al., 2021).

Declaration of competing interest

The authors declare that they have no known competing financial interests or personal relationships that could have appeared to influence the work reported in this paper.

Acknowledgments

This work was supported by the Russian Science Foundation under the grant 20-41-04404 issued to the Institute of Applied Mechanics of Russian Academy of Sciences. Third author acknowledges the financial support of the German Research Foundation grant (AL 341/51-1).

References

Altan, B., Aifantis, E., 1997. On some aspects in the special theory of gradient elasticity. J. Mech. Behav. Mater. 8 (3), 231–282.

Anagnostou, D., Gourgiotis, P., Georgiadis, H., 2015. The Cerruti problem in dipolar gradient elasticity. Math. Mech. Solids 20 (9), 1088–1106.

Andreaus, U., dell'Isola, F., Giorgio, I., Placidi, L., Lekszycki, T., Rizzi, N., 2016. Numerical simulations of classical problems in two-dimensional (non) linear second gradient elasticity. Int. J. Eng. Sci. 108, 34–50.

Askes, H., Aifantis, E., 2011. Gradient elasticity in statics and dynamics: an overview of formulations, length scale identification procedures, finite element implementations and new results. Int. J. Solids Struct. 48 (13), 1962–1990.

Barber, J., 2002. Elasticity. Springer.

Charalambopoulos, A., Polyzos, D., 2015. Plane strain gradient elastic rectangle in tension. Arch. Appl. Mech. 85 (9), 1421–1438.

Charalambopoulos, A., Tsinopoulos, S., Polyzos, D., 2020. Plane strain gradient elastic rectangle in bending. Arch. Appl. Mech. 90 (5), 967–986.

Cordero, N., Forest, S., Busso, E., 2016. Second strain gradient elasticity of nano-objects. J. Mech. Phys. Solids 97, 92–124.

dell'Isola, F., della Corte, A., Giorgio, I., 2017. Higher-gradient continua: The legacy of piola, mindlin, sedov and toupin and some future research perspectives. Math. Mech. Solids 22 (4), 852–872.

dell'Isola, F., Sciarra, G., Vidoli, S., 2009. Generalized Hooke's law for isotropic second gradient materials. Proc. R. Soc. Math. Phys. Eng. Sci. 465 (2107), 2177–2196.

Eremeyev, V., Cazzani, A., dell'Isola, F., 2021. On nonlinear dilatational strain gradient elasticity. Contin. Mech. Thermodyn. 1–35.

Eremeyev, V., Lurie, S., Solyaev, Y., dell'Isola, F., 2020. On the well posedness of static boundary value problem within the linear dilatational strain gradient elasticity. Z. Angew. Math. Phys. 71 (6), 1–16.

Eremeyev, V., Rosi, G., Naili, S., 2019. Comparison of anti-plane surface waves in strain-gradient materials and materials with surface stresses. Math. Mech. Solids 24 (8), 2526–2535.

Eshel, N., Rosenfeld, G., 1970. Effects of strain-gradient on the stress-concentration at a cylindrical hole in a field of uniaxial tension. J. Eng. Math. 4 (2), 97–111.

Georgiadis, H., Anagnostou, D., 2008. Problems of the Flamant–Boussinesq and Kelvin type in dipolar gradient elasticity. J. Elast. 90 (1), 71–98.

Giorgio, I., 2016. Numerical identification procedure between a micro-Cauchy model and a macro-second gradient model for planar pantographic structures. Z. Angew. Math. Phys. 67 (4), 1–17.

Giorgio, I., dell'Isola, F., Steigmann, D., 2018a. Axisymmetric deformations of a 2nd grade elastic cylinder. Mech. Res. Commun. 94, 45–48.

Giorgio, I., Harrison, P., dell'Isola, F., Alsayednoor, J., Turco, E., 2018b. Wrinkling in engineering fabrics: a comparison between two different comprehensive modelling approaches. Proc. R. Soc. Math. Phys. Eng. Sci. 474 (2216), 20180063.

Gourgiotis, P., Georgiadis, H., 2009. Plane-strain crack problems in microstructured solids governed by dipolar gradient elasticity. J. Mech. Phys. Solids 57 (11), 1898–1920.

Gourgiotis, P., Georgiadis, H., 2011. The problem of sharp notch in couple-stress elasticity. Int. J. Solids Struct. 48 (19), 2630–2641.

Gourgiotis, P., Sifnaiou, M., Georgiadis, H., 2010. The problem of sharp notch in microstructured solids governed by dipolar gradient elasticity. Int. J. Fract. 166 (1–2), 179–201.

Gourgiotis, P., Zisis, T., Georgiadis, H., 2018. On concentrated surface loads and Green's functions in the Toupin–Mindlin theory of strain-gradient elasticity. Int. J. Solids Struct. 130, 153–171.

Gurtin, M., 1962. On Helmholtz's theorem and the completeness of the Papkovich-Neuber stress functions for infinite domains. Arch. Ration. Mech. Anal. 9, 225–233.

Kołodziej, J.A., Zielinski, A., 2009. Boundary Collocation Techniques And Their Application In Engineering. WIT Press.

Lazar, M., 2013. The fundamentals of non-singular dislocations in the theory of gradient elasticity: Dislocation loops and straight dislocations. Int. J. Solids Struct. 50 (2), 352–362.

Lazar, M., 2021. Incompatible strain gradient elasticity of mindlin type: screw and edge dislocations. Acta Mech. 232 (9), 3471–3494.
Lazar, M., Agiasofitou, E., Böhlke, T., 2021. Mathematical modeling of the elastic properties of cubic crystals at small scales based on the Toupin–Mindlin anisotropic first strain gradient elasticity. Contin. Mech. Thermodyn. 1–30.
Lazar, M., Maugin, G.A., 2005. Nonsingular stress and strain fields of dislocations and disclinations in first strain gradient elasticity. Int. J. Eng. Sci. 43 (13–14), 1157–1184.
Lazar, M., Maugin, G., 2006. A note on line forces in gradient elasticity. Mech. Res. Commun. 33 (5), 674–680.
Lazar, M., Polyzos, D., 2015. On non-singular crack fields in Helmholtz type enriched elasticity theories. Int. J. Solids Struct. 62, 1–7.
Lurie, A., 2005. Theory Of Elasticity. Springer-Verlag Berlin Heidelberg, Berlin.
Lurie, S., Belov, P., Volkov-Bogorodsky, D., Tuchkova, N., 2006. Interphase layer theory and application in the mechanics of composite materials. J. Mater. Sci. 41 (20), 6693–6707.
Lurie, S., Kalamkarov, A., Solyaev, Y., Volkov, A., 2021. Dilatation gradient elasticity theory. Eur. J. Mech. A/Solids 88, 104258.
Lurie, S., Volkov-Bogorodsky, D., Leontiev, A., Aifantis, E., 2011. Eshelby's inclusion problem in the gradient theory of elasticity: applications to composite materials. Int. J. Eng. Sci. 49 (12), 1517–1525.
Ma, H., Hu, G., Wei, Y., Liang, L., 2018. Inclusion problem in second gradient elasticity. Int. J. Eng. Sci. 132, 60–78.
Madeo, A., Ghiba, I., Neff, P., Münch, I., 2016. A new view on boundary conditions in the Grioli-Koiter-Mindlin-Toupin indeterminate couple stress model. Eur. J. Mech. A/Solids 59, 294–322.
Mindlin, R., 1936. Note on the Galerkin and Papkovitch stress functions. Bull. Am. Math. Soc. 42 (6), 373–376.
Mindlin, R., 1964. Micro-structure in linear elasticity. Arch. Ration. Mech. Anal. 16 (1), 51–78.
Mindlin, R., Tiersten, H., 1962. Effects of couple-stresses in linear elasticity. Arch. Ration. Mech. Anal. 11 (1), 415–448.
Morse, P., Feshbach, H., 1953. Methods Of Theoretical Physics, Part II. McGraw-Hill, New York.
Nazarenko, L., Glüge, R., Altenbach, H., 2021. Uniqueness theorem in coupled strain gradient elasticity with mixed boundary conditions. Contin. Mech. Thermodyn. 1–14.
Park, S., Gao, X.-L., 2008. Variational formulation of a modified couple stress theory and its application to a simple shear problem. Z. Angew. Math. Phys. 59 (5), 904–917.
Placidi, L., El Dhaba, A., 2017. Semi-inverse method à la Saint-Venant for two-dimensional linear isotropic homogeneous second-gradient elasticity. Math. Mech. Solids 22 (5), 919–937.
Quartapelle, L., 2013. Numerical Solution Of The Incompressible Navier-Stokes Equations. In: International Series of Numerical Mathematics, vol. 113, Birkhäuser.
Reiher, J., Giorgio, I., Bertram, A., 2017. Finite-element analysis of polyhedra under point and line forces in second-strain gradient elasticity. J. Eng. Mech. 143 (2), 04016112.
Sciarra, G., Vidoli, S., 2012. The role of edge forces in conservation laws and energy release rates of strain-gradient solids. Math. Mech. Solids 17 (3), 266–278.
Sciarra, G., Vidoli, S., 2013. Asymptotic fracture modes in strain-gradient elasticity: Size effects and characteristic lengths for isotropic materials. J. Elast. 113 (1), 27–53.
Solyaev, Y., Lurie, S., 2021. Trefftz collocation method for two-dimensional strain gradient elasticity. Int. J. Numer. Methods Eng. 122 (3), 823–839.
Solyaev, Y., Lurie, S., Korolenko, V., 2019. Three-phase model of particulate composites in second gradient elasticity. Eur. J. Mech. A/Solids 78, 103853.
Sprössig, W., 2010. On Helmholtz decompositions and their generalizations – an overview. Math Methods Appl. Sci. 33 (4), 374–383.
Toupin, R.A., 1964. Theories of elasticity with couple-stress. Arch. Ration. Mech. Anal. (ISSN: 00039527) 17 (2), 85–112.
Uflyand, Y., 1965. Survey Of Articles On The Applications Of Integral Transforms In The Theory Of Elasticity. Air Force Office of Scientific Research, Air Research and Development Command, United States Air Force, Washington, D.C..
Vasiliev, V., Lurie, S., Salov, V., 2021a. On the flamant problem for a half-plane loaded with a concentrated force. Acta Mech. 232 (5), 1761–1771.
Vasiliev, V., Lurie, S., Solyaev, Y., 2021b. New approach to failure of pre-cracked brittle materials based on regularized solutions of strain gradient elasticity. Eng. Fract. Mech. 258, 108080.
Yang, H., Timofeev, D., Giorgio, I., Müller, W., 2020. Effective strain gradient continuum model of metamaterials and size effects analysis. Contin. Mech. Thermodyn. 1–23.
Zhao, J., Pedroso, D., 2008. Strain gradient theory in orthogonal curvilinear coordinates. Int. J. Solids Struct. 45 (11–12), 3507–3520.
Zieliński, A., 1995. On trial functions applied in the generalized Trefftz method. Adv. Eng. Softw. 24 (1–3), 147–155.